JMA's C-band dual-polarization Doppler weather radars with SSPAs

Naoki Tsukamoto[1], Hiroshi Yamauchi[1], Hidehiro Okumura[2], Akihito Umehara[1] and Yusuke Kajiwara[1]

1 Japan Meteorological Agency (JMA), Tokyo, Japan

2 Narita Aviation Weather Service Center, JMA, Chiba, Japan

Abstract

In March 2016, the Japan Meteorological Agency (JMA) began to operate C-band dual-polarization Doppler weather radars with solid-state power amplifiers (SSPAs) at Kansai International Airport and Tokyo International Airport. The new radars feature a dual-polarization function and SSPA pulse compression.

Observational data improvement is a major objective associated with the WMO Integrated Global Observing System (WIGOS). The dual-polarization function is expected to help improve quantitative precipitation estimation (QPE) and quality control (QC), as well as to support the provision of new products that allow identification of precipitation as rain, snow or hail. JMA is currently evaluating the accuracy of the new radar observation based on comparison with surface observation data.

SSPA usage and the adoption of pulse compression reduce the radar's peak power from the 200 kW of conventional klystrons to just 10 kW. The set-up also supports narrow bandwidth and improved signal detection capability, thereby contributing to the mitigation of interference with 5 GHz-band radio LAN (RLAN).

The significant advantages of dual-polarization Doppler weather radar with SSPA will be highlighted via analysis of observational data during the 2016 rainy season.

1. Introduction

In Japan, weather radar data are widely used for a variety of purposes including weather monitoring/prediction, water resource management and aviation safety. Such information therefore plays a pivotal role in protecting people from severe storms.

The Japan Meteorological Agency (JMA) deploys nine Doppler Radars for Airport Weather (DRAWs) to support aviation safety. The first DRAW was installed at Kansai International Airport in 1994, and has remained operational since then.

In 2016, the two DRAWs at Kansai International Airport and Tokyo International Airport (Haneda) were replaced with new SP-DRAW (solid-state polarimetric DRAW) types featuring SSPAs and dual polarization. Another SP-DRAW is scheduled for installation at Narita International Airport in 2016.

The adoption of solid-state transmitters in DRAWs is based on the serious threat from interference caused by telecommunication devices (e.g., RLAN) to weather radars worldwide (Elena et al. 2015). The shortage of 5-GHz frequency band (C-band) space allocated to weather radars and RLAN is also a problem in Japan.

To solve this problem, Japan's radio regulatory authority is taking measures to separate frequency bands allocated to weather radar and RLAN services. The resulting radio frequency reallocation plan for weather radars in Japan will be based on nine channels with increments of 5 MHz within narrow band-width areas, as opposed to the conventional allocation plan based on channels with increments of 10 MHz. Accordingly, there is a need to reduce the bandwidth, unwanted emissions and peak power of weather radars.

During the period of transition from the conventional channel allocation plan to the new reallocation plan, radio frequency channels may need to be temporarily changed for some weather radars to prevent interference with other radars. However, changing the transmission frequency of conventional radars requires very expensive waveguide filters that allow high-power handling and very-narrow-band operation. In contrast, the operation radio frequency of SP-DRAW can be readily changed because no such filter is required.

To reduce operational costs, SP-DRAW also allows savings in areas such as consumable parts (through factors such as elimination of the need to use magnetron or klystron) and requires less space and electric power.

2. Characteristics of SP-DRAW

2.1 Purposes of SP-DRAW

Figure 1 shows the Haneda Airport SP-DRAW, whose main roles are to detect low-level wind shear (LLWS, including microbursts (MB) and horizontal shear lines (SL)) at/around the airport and to alert pilots if threshold levels are exceeded (Fig. 2). Clutter signals can reduce the quality of radar echo and consequently affect the reliability of LLWS detection.

The SP-DRAW system can be used to identify weather and non-weather echoes using dual-polarization parameters, while conventional Doppler weather radar data may be affected by unintentional removal of weather echo because a high QC threshold is adopted to reduce clutter contamination. The introduction of SP-DRAWs has enabled the collection of high-quality Doppler velocity data without clutter contamination even in weak echo regions, which improve accuracy for identification of areas of sudden wind

change. This has led to better accuracy in LLWS detection, which is a major purpose of aviation weather radar usage.

Fig. 1 Haneda Airport SP-DRAW tower

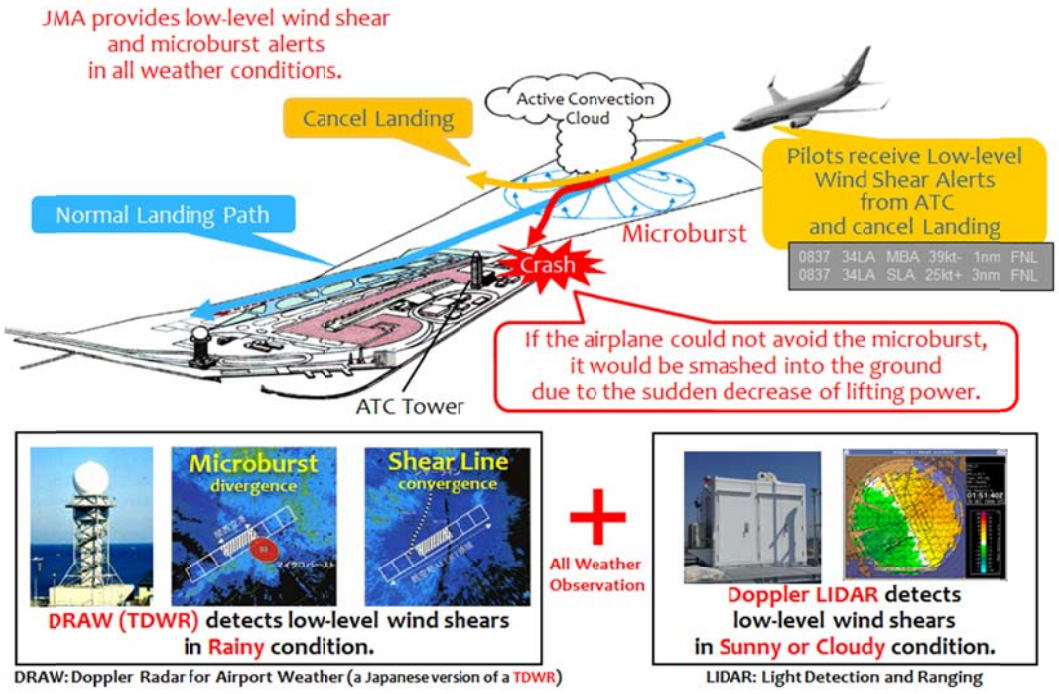

Fig. 2 Roles of SP-DRAW

2.2 Specifications of SP-DRAW and related operating parameters

Table 1 shows the specifications and operating parameters of SP-DRAW compared with those of conventional DRAW.

Table 1. Specifications/operating parameters of SP-DRAW and conventional DRAW

	SP-DRAW	Conventional DRAW
Frequency	5,360 MHz	5,280 MHz
Transmitters	GaN Power FET	Klystron
Peak transmitter power	5 kW for both H and V	200 kW
Antenna diameter	7 m (parabolic)	7 m
Beam width	< 0.7°	< 0.7°
Antenna gain	> 47 dBi	> 47 dBi
Signal min.	< -110 dBm	< -110 dBm
Side lobe level	< -27 dB	< -27 dB
Range side lobe level	< -55 dB	
Range gate spacing	150 m	150 m
Radome diameter	11 m	11 m
Antenna rotation rate	4.2 rpm (EL = < 9.2°)	4 rpm
	7 rpm (EL > 9.2°)	
Samples (hits)	18 – 29	32
Azimuth spacing	0.7°	0.7°
Pulse repetition frequency	1,040/832 Hz (EL = < 9.2°)	1,120/840 Hz
	1,365/1,092 Hz (EL > 9.2°)	
Pulse width	1 μs (range < 12 km)	1 μs
	64 μs (range >= 12 km)	
Transmission mode	Dual (simultaneous)	Single (horizontal)
Observation parameters	Z, V, W, Z_{DR}, ρ_{HV}, Φ_{DP}	Z, V, W

Transmission radio frequency can be set to any value between 5,330 and 5,370 MHz. As high-power gallium nitride FETs are used for SSPAs, peak SP-DRAW transmitter power can reach 5 kW for each (H/V) polarized wave. The bandwidth of transmitted waves is quite narrow, and leakage to the adjacent channel is substantially suppressed.

Pulse widths can be set freely from 1 to 200 μs. JMA operationally uses values of 1 and 64 μs for short and long pulses, respectively. A pulse compression technique

involving the use of frequency chirp is adopted in long-pulse observation. SP-DRAW also provides the ability to adjust the phase of drive signals for horizontal and vertical wave transmission, which is important for simultaneous transmission and reception observation mode operation as reported by Hubbert et al. (2010). Related adjustment was performed using a standard horn antenna in the far field of SP-DRAW's antenna during the installation period.

The SP-DRAW parabolic antenna is shown in Fig. 3.

This 7-m antenna allows the generation of sharp beam patterns appropriate for detection of LLWS near the surface. In addition, to enable the derivation of high-quality Z_{DR} and ρ_{HV} values, a cross-polarization isolation value exceeding 35 dB is secured without radome; this has been proven to exceed 34 dB with radome based on evaluation using the method proposed by Frech et al. (2012). The antenna rotation rate can be set at up to 7 rpm for configuration of optimal scan sequencing to reduce observation times.

Due to the trade-off between the antenna rotation rate and radar data quality, rotation rates differ between lower-elevation scans (which are more easily affected by clutter) and higher-elevation scans (which are focused on fast scanning).

For lower-elevation scans, an antenna rotation rate of 4.2 rpm is set in consideration of ground clutter removal performance. For higher-elevation scans with less ground clutter contamination, the rate is set as 7 rpm with high pulse repetition frequency.

Fig. 3 SP-DRAW antenna

2.3 Observation procedure

The major SP-DRAW processes for LLWS detection involve MB identification every minute and SL identification every five minutes. These forms of detection are based on Doppler velocity data obtained using the dual-PRF technique and the hybrid multi-PRI method (Yamauchi et al. 2006).

MBs are detected using a plan position indicator (PPI) at the lowest elevation angle (0.7°), while SLs are detected using PPIs at two lower elevation angles (0.7 and 1.1°). The need to scan PPIs at 0.7 and 1.1° individually represents a constraint in the planning scan sequence for SP-DRAW. Meanwhile, scanning of PPIs at higher elevation angles and range height indicator (RHI) operation are conducted during spare time for observation of precipitation and wind in and around the airport. Scanning is performed to obtain RHI data, which are especially useful for monitoring the vertical structures of precipitation and wind on the approach to the airport parallel to its main runway. PPI scanning at an elevation of 90° (known as bird-bath scanning), which produces data used for calibration of dual-polarization parameters and early detection of system anomalies, is conducted.

Thus, the five-minute scan sequence shown in Fig. 4 is implemented for SP-DRAW.

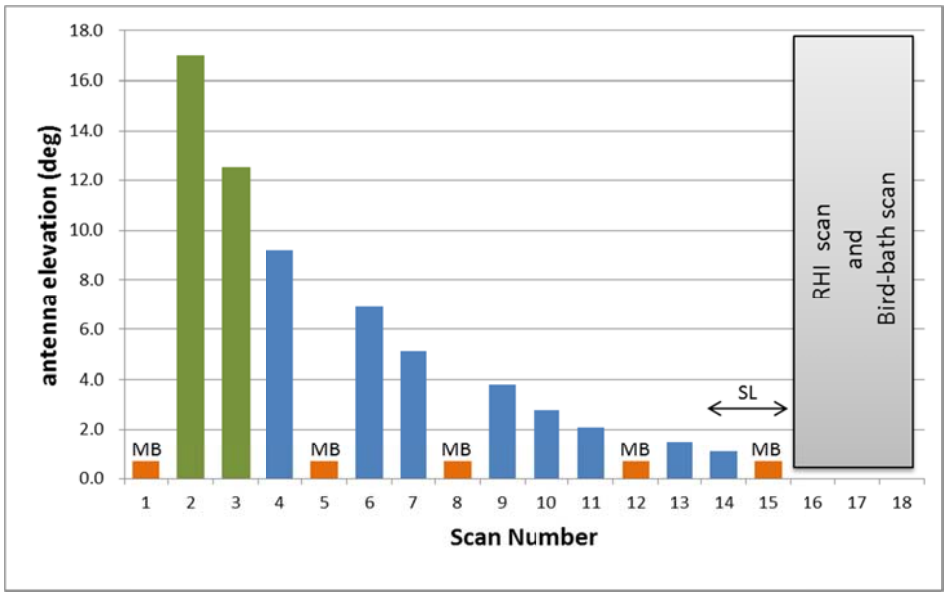

Fig. 4 Five-minute antenna scan sequence

Long pulse width observation and pulse-compression techniques are used to ensure the requisite sensitivity of SP-DRAW, as the peak transmitter power for each

polarization is 5 kW (i.e., only 1/40th of those of conventional radars with a klystron). A 1-μs pulse is also used to complement observation within truncated ranges corresponding to the time of long-pulse emission (Fig. 5). In long-pulse-width observation, a value of 64 μs is adopted for better sensitivity both in long- and short-pulse observation ranges (Fig. 6). As a result, the average power of SP-DRAW is 1.5 times better than that of conventional DRAW (1 μs, 200 kW). The overall horizontal and vertical average transmitted power from the new radar system is three times that of conventional radar, but its overall electricity consumption is 20 percent lower.

As the truncated range for the long pulse width (64 μs) is equal to 12 km with some margin, a sensitivity gap is observed at 12 km. However, this does not pose problems in practical use because short pulses (1 μs) have enough power for detection of meteorological echoes near the radar site (Fig. 7).

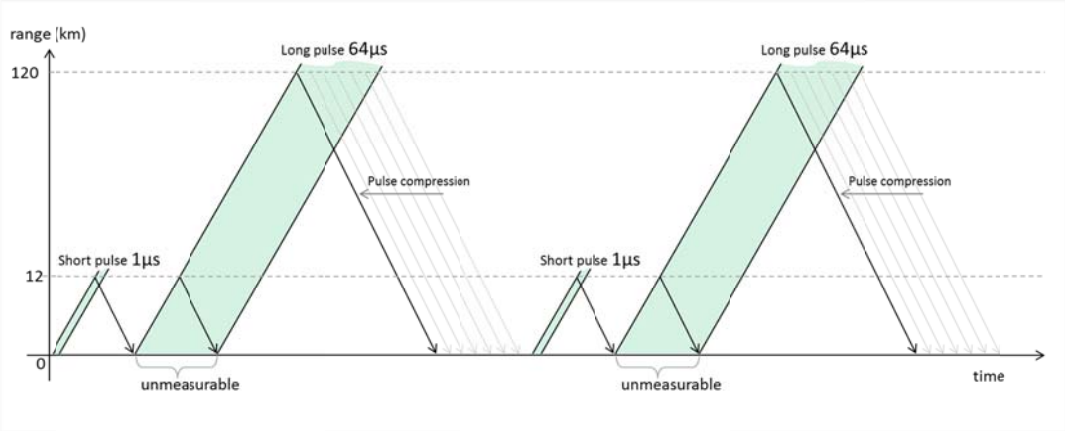

Fig. 5 Relationship between pulse width and measurable area

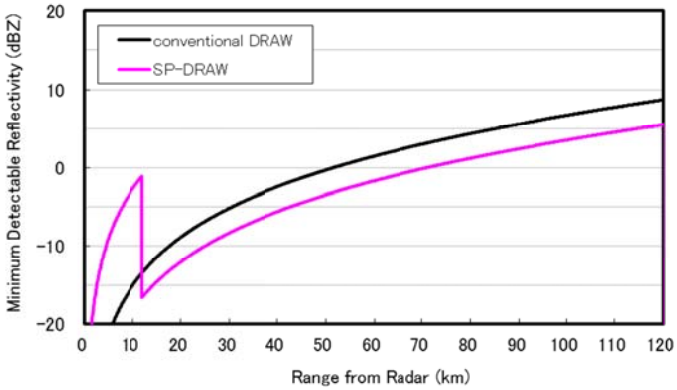

Fig. 6 Relationship between minimum detectable reflectivity and range from radar for conventional DRAW (black line) and SP-DRAW (purple line)

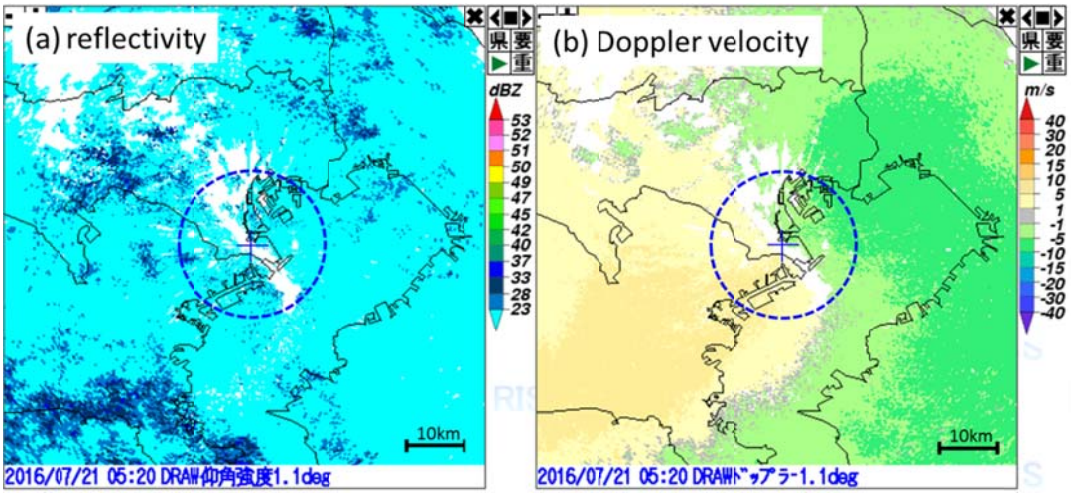

Fig. 7 PPI plots of (a) reflectivity and (b) Doppler velocity for weak weather echoes at an elevation angle of 1.1°. The blue dotted circle indicates the short-pulse observation region.

2.4 Improvement of radar system stability

The transmitter, receiver, signal processor and antenna controller are shown in Fig. 8. Figure 9 gives an overview of the system including the antenna, transmitter, receiver and signal processor.

The SP-DRAW system is designed with high redundancy to ensure stable provision of information to flights. The transmitter consists of eight SSPA modules for horizontal polarized waves and another eight for vertical polarized waves, and transmits waves synthesized from the output of these sixteen modules. In the event of a module malfunction, operation can be continued on the basis of radar equation calculation with reduced transmission power.

Two receiver/signal processor sets are operated in the form of a duplex system. These devices are used to generate drive signals and receive/process echo signals. The active system of the devices outputs observation data (the moment data) into two data processors used to conduct LLWS detection, which are operated in the form of a dual system.

Two antenna controllers are operated in the form of a duplex system.

As SP-DRAW is premised on continuous system operation, it includes functions for system stability checking and quality maintenance in day-to-day operation. To monitor system status in daily application, SP-DRAW constantly monitors transmission power and receiver sensitivity using test signals.

As mentioned previously, SP-DRAW monitors Z_{DR} and Φ_{DP} using bird-bath scanning to enable detection of system errors and misalignments across the whole system.

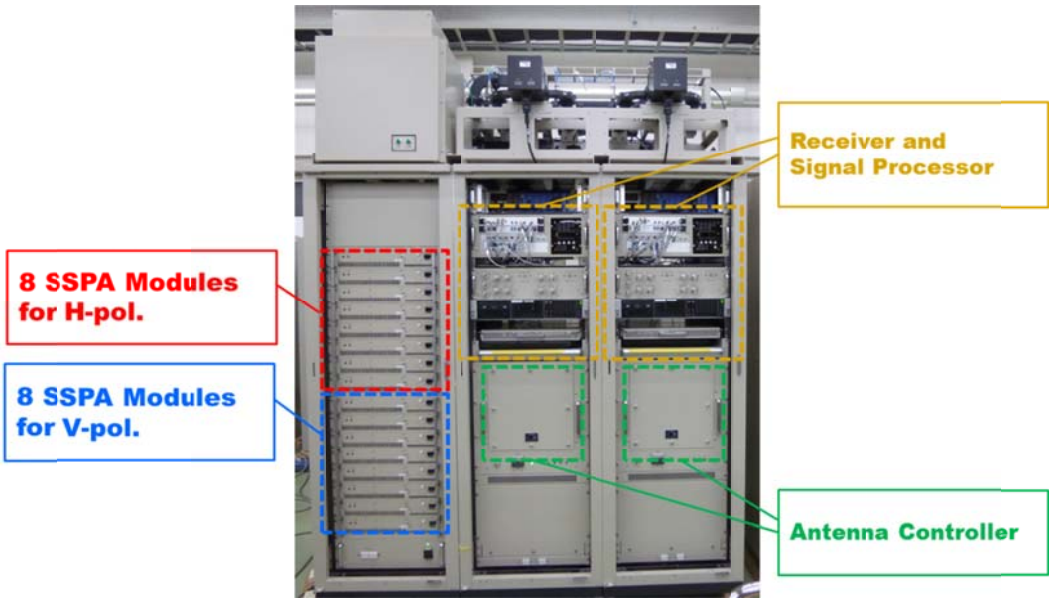

Fig. 8 Transmitter, receiver, signal processor and antenna controller

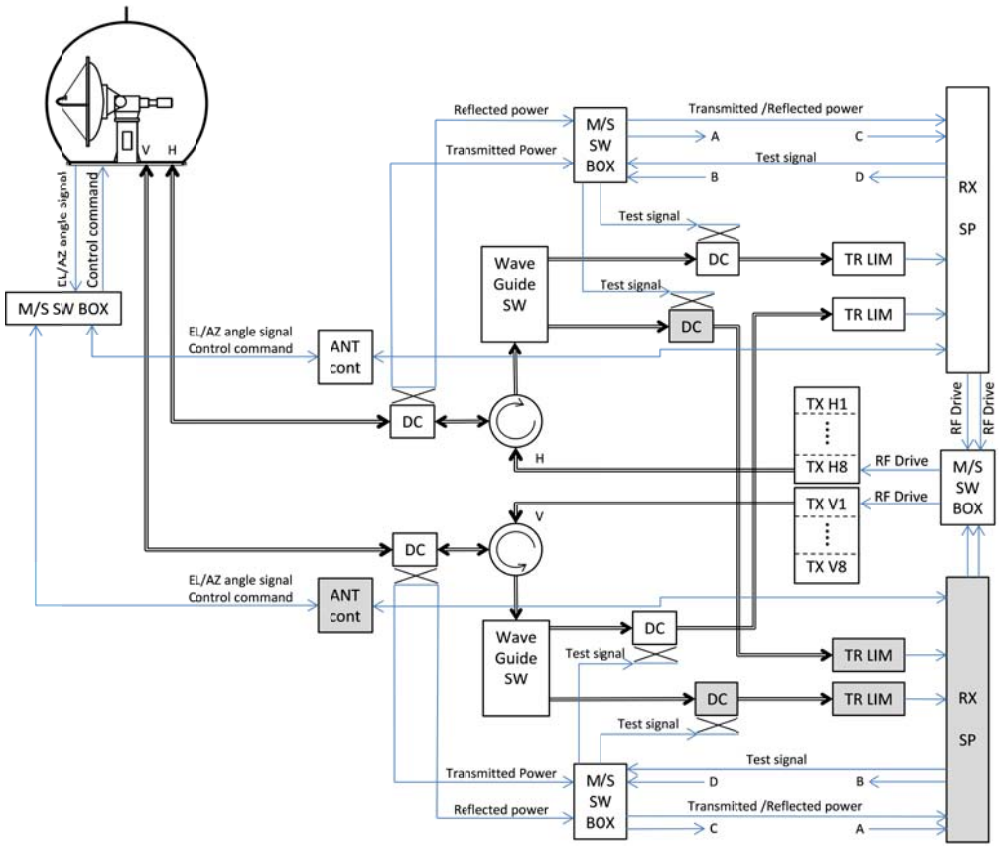

Fig. 9 Block diagram of SP-DRAW

2.5 Quality control methods

To improve the quality of Doppler velocity data at the lowest elevation angle, which are essential for LLWS detection, SP-DRAW incorporates a new clutter discrimination algorithm for which dual-polarization parameters are utilized. Ground clutter (GC) and moving clutter such as ships and wind turbines impair the quality of Doppler velocity data and cause false LLWS detection. Although the moving target indicators (MTIs) used for conventional Doppler radars help to mitigate GC to a certain degree, they have no effect in relation to moving clutter. Meanwhile, dual-polarization parameters can be used to efficiently distinguish both GC and moving clutter. The use of MTIs sometimes also results in the removal or attenuation of weather echo. To avoid this side effect, MTI processing data should be applied only for bins contaminated by GC, and normal processing data (NOR) should be applied for pure weather echo.

Figure 10 shows a flow chart of the clutter discrimination algorithm for which dual-polarization parameters are used. This involves the utilization of clutter phase alignment (CPA; Hubbert et al. 2009) and the texture of the differential phase $S(\Phi_{DP})$ in

addition to the conventional clutter suppression rate (CSR) derived from MTI processing to determine whether individual bins include clutter. $S(\Phi_{DP})$ is the root mean square error (RMSE) of fitting for Φ_{DP} values of five bins in a radial row. The parameter is small for precipitation echo and large for clutter. CPA and $S(\Phi_{DP})$ are calculated for both NOR processing data and MTI processing data.

If the CSR, CPA(NOR) and $S(\Phi_{DP})$(NOR) values for a certain bin are below the set thresholds, the bin is assumed to be uncontaminated by clutter [flag 0]. If the CSR, CPA(MTI) and $S(\Phi_{DP})$(MTI) values for the bin are below the set thresholds, the bin is assumed to be contaminated by weak ground clutter whose effects are well mitigated by MTI [flag 1]. Otherwise, the bin is assumed to be contaminated by strong ground clutter or moving clutter whose effects are difficult to mitigate with MTI [flag 2]. Normal data, MTI data and invalid data are applied for bins flagged with [0], [1] and [2], respectively. The threshold values can be adjusted, and JMA is currently evaluating the values used for optimization to avoid significant effects on weather echo.

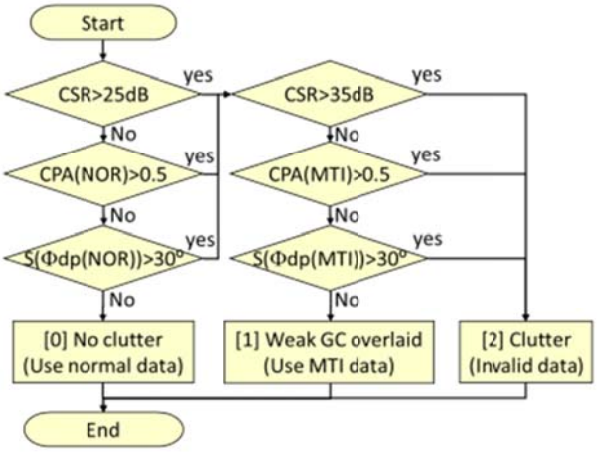

Fig. 10 Clutter discrimination algorithm

3. SP-DRAW observation data

As part of polarimetric performance verification, the JMA is evaluating the accuracy of precipitation estimates using SP-DRAW dual-polarization parameters based on comparison with data from weighing rain gauges (WGs) installed at five special surface observation sites around each SP-DRAW. This section details the preliminary results of evaluation for a heavy rainfall event that produced hourly precipitation of up to 57 mm at the Tateno surface observation site 65 km northeast of the Haneda SP-DRAW on 14 July 2016. Figure 11 shows PPIs of reflectivity Z and the specific differential phase Kdp

as observed via the Haneda SP-DRAW. In line with the method of Yamauchi et al. (2012), which involves the use of coefficients proposed by Bringi and Chandrasekar (2001), the rain rate R(Kdp, Z_corr) is estimated using Kdp and attenuation-corrected reflectivity Z_corr. Conventional rain rate estimation R(Z) is also conducted. Figures 12 (a) and (b) show distributions of estimated rain rates R(Z) and R(Kdp, Z_corr), respectively. The latter shows heavy rain areas more clearly.

Figure 13 shows a time-series representation of rain rates as observed using weighing rain gauge data R(WG), R(Z) and R(Kdp, Z_corr) at the Tateno site. In consideration of the time taken for raindrops to fall from a distance of 1 km above the ground, the times of R(Z) and R(Kdp, Z_corr) are delayed by 4 minutes assuming a descent rate of 4 m/s. While correspondence between R(Kdp, Z_corr) and R(WG) is seen, R(Z) represents significant underestimation of the rain rate. The one-hour cumulative value of R(Kdp, Z_corr) from 16:57 to 17:57 is 11% underestimated against R(WG), while that of R(Z) is 74% underestimated.

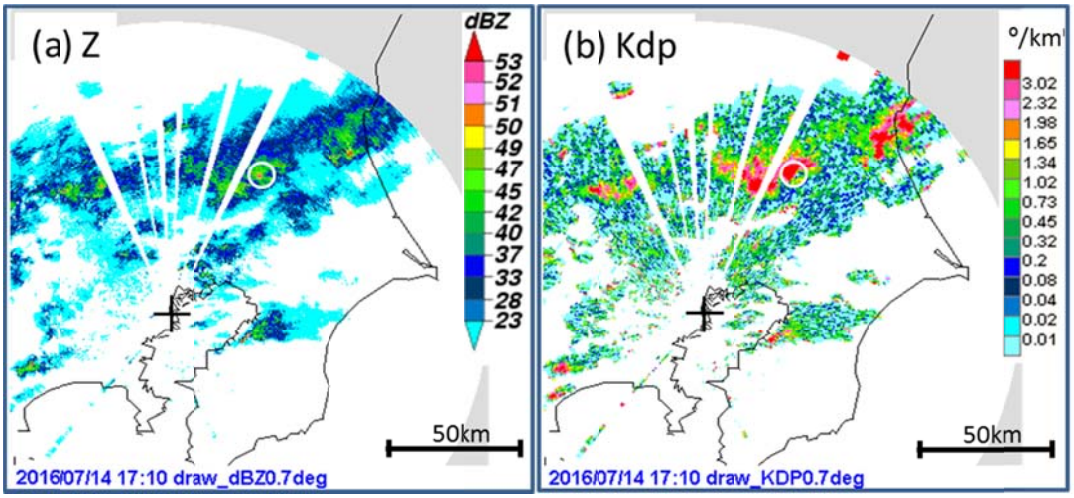

Fig. 11 PPI plots of (a) reflectivity and (b) Kdp as observed using the Haneda DRAW with an elevation angle of 0.7º at 1710 JST on 14 July 2016. The black crosses and white circles indicate the locations of the Haneda DRAW and the Tateno site, respectively.

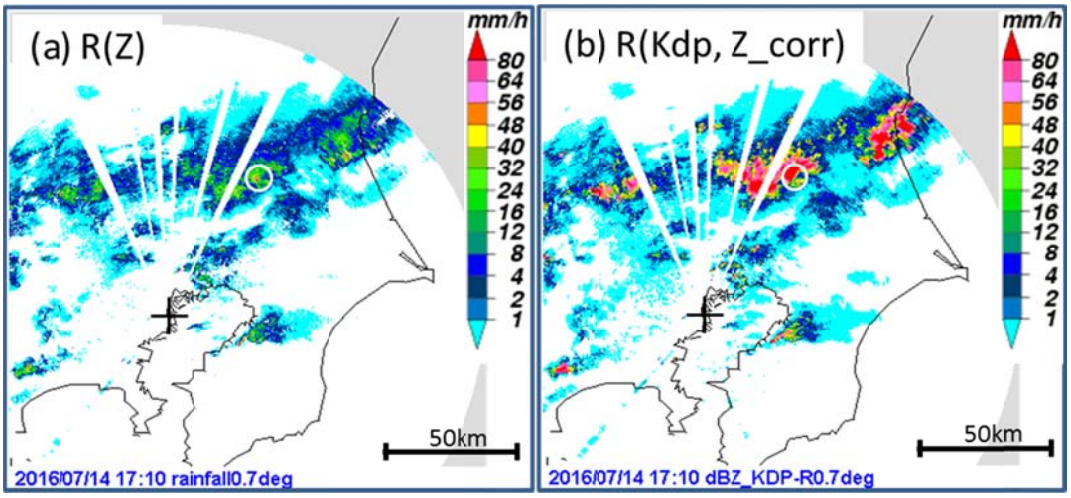

Fig. 12 As per Fig. 11, but with rain rate distribution estimated using (a) R(Z) and (b) R(Kdp, Z_corr)

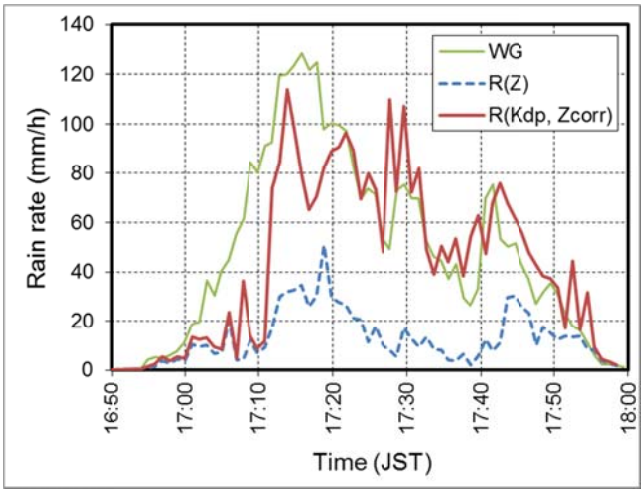

Fig. 13 Time-series representation of rain rates observed using weighing rain gauges (thin green line) and estimated using R(Z) (dotted blue line) and R(Kdp, Z_corr) (thick red line)

4. Summary and future plans

SP-DRAW guarantees adequate radar observation data quality even with high-speed antenna scanning. The results of the study confirmed the expected level of observational capacity for practical operation in very strong to very weak echo areas.

In response to growing demand for high-quality radar data, the SP-DRAW quality assurance system now includes a built-in independent checking function and continuous quality monitoring based on bird-bath scanning to detect issues during

operation.

High-quality data and frequent observation are essential for the early detection of severe storms, which is one of JMA's goals.

In relation to effective radio frequency usage, solid-state transmitters are very useful because they support:

- achievement of balance between peak power reduction and high data quality;
- mitigation of unexpected emissions against adjacent channels; and
- simple frequency changes.

With this approach, electricity consumption is 20% less than with conventional radar.

Observational data improvement is a major objective associated with the WMO Integrated Global Observing System (WIGOS). To support the achievement of this goal, JMA will share lessons learned from its adoption of new-generation weather radars with NMHSs.

References

Bringi, V. N. and V. Chandrasekar, 2001: Polarimetric Doppler weather radar: principles and applications, Cambridge University Press, 636pp.

Hubbert, J., M. Dixon, S. Ellis, and G. Meymaris, 2009: Weather radar ground clutter. Part I: Identification, modeling, and simulation. *J. Atmos. Oceanic Technol.*, **26**, 1165–1180.

Hubbert, J., S. Ellis, M. Dixon, and G. Meymaris, 2010: Modeling, error analysis, and evaluation of dual-polarization variables obtained from simultaneous horizontal and vertical polarization transmit radar. Part I: modeling and antenna errors. *J. Atmos. Oceanic Technol.*, **27**, 1583–1598.

Frech, M., B. Lange, T. Mammen, J. Seltmann, C. Morehead and J. Rowan, 2013: Influence of a radome on antenna performance. J. Atmos. Oceanic Technol., **30**, 313–324.

Saltikoff, E., J. Cho, P. Tristant, A. Huuskonen, L. Allmon, R. Cook, E. Becker, and P. Joe, 2015: The Threat to Weather Radars by Wireless Technology. *Bull. Amer. Meteor. Soc.,* doi:10.1175/BAMS-D-15-00048.1, in press

Yamauchi, H., O. Suzuki and K. Akaeda, 2006: A hybrid multi-PRI method to dealias Doppler velocities. *SOLA*, **2**, 92–95.

Yamauchi, H., A. Adachi, O. Suzuki and T. Kobayashi, 2012: Precipitation estimate of a heavy rain event using a C-band solid-state polarimetric radar, Extended abstract, 7th European Conf. on Radar in Meteorol. and Hydrol., Toulouse, France, 201SP.